

SGEN: Single-cell Sequencing Graph Self-supervised Embedding Network

Ziyi Liu¹, Minghui Liao¹, Fulin Luo^{2*} and Bo Du^{1†}

¹National Engineering Research Center for Multimedia Software, Institute of Artificial Intelligence, School of Computer Science, and Hubei Key Laboratory of Multimedia and Network Communication Engineering, Wuhan University, Wuhan, 430072, China

²State Key Laboratory of Information Engineering in Surveying, Mapping, and Remote Sensing, Wuhan University, Wuhan 430079, China

Abstract

Single-cell sequencing has significant role to explore biological processes such as embryonic development, cancer evolution and cell differentiation. These biological properties can be presented by two-dimensional scatter plot. However, single-cell sequencing data generally has very high dimensionality. Therefore, dimensionality reduction should be used to process the high dimensional sequencing data for 2D visualization and subsequent biological analysis. The traditional dimensionality reduction methods, which don't consider the structure characteristics of single-cell sequencing data, are difficult to reveal the data structure in the 2D representation. In this paper, we develop a 2D feature representation method based on graph convolutional networks (GCN) for the visualization of single-cell data, termed single-cell sequencing graph embedding networks (SGEN). This method constructs the graph by the similarity relationship between cells and adopts GCN to analyze the neighbor embedding information of samples, which makes the similar cell closer to each other on the 2D scatter plot. The results show SGEN achieves obvious 2D distribution and preserves the high-dimensional relationship of different cells. Meanwhile, similar cell clusters have spatial continuity rather than relying heavily on random initialization, which can reflect the trajectory of cell development in this scatter plot.

1 Introduction

Complex biological tissues are composed of functionally diverse, heterogeneous populations of cells. Single-cell sequencing [Gawad *et al.*, 2016], which gives all the transcriptome or genome information of individual cell rather than bulk samples, provides cell-specific insights, including monitoring abnormal cells [Franke *et al.*, 2006], tracking cell development [Hubert and Arabie, 1985], and detecting cell responses to environmental disturbances [William *et al.*, 1971].

It is now widely used in many biological fields to analyze the biological status of individual cells, including cancer biology [Wang *et al.*, 2014], immunology [Stubbington *et al.*, 2017], and metagenomics [Yoon *et al.*, 2011]. Single-cell sequencing can also identify cells with different gene expression in different environments to explore the causes of differential expression [Grün *et al.*,].

In single-cell sequencing data, each cell is described as a vector consisting of the expression values of all genes. The data from single-cell sequencing are large in volume and high-dimensional, as each cell contains tens of thousands of gene expression values and the number of cells of each batch amounts to hundreds of thousands. In the subsequent data analysis, it is very time-consuming and inconvenient to operate such a huge matrix mathematically, and the redundancy caused by many strongly correlated genes results in the waste of computing resources, so an appropriate algorithm should be constructed to reduce the dimensions of the single-cell sequencing data. The other purpose of dimensionality reduction is visualization with a 2D scatter plot, where cells in similar biological status presented on the 2D scatter plot are closer to each other than those in diverse biological status. The high volume and high dimension of the single-cell sequencing data pose challenges to existing dimensionality reduction algorithms.

Linear dimensionality reduction algorithms, such as the principal component analysis (PCA) [Moon *et al.*, 2017], do not work well in 2 or 3 dimensions on capturing the original structural information from high dimension for the inherent non-linearity of single-cell sequencing data. Because of the high efficiency of PCA, it is often used as a pre-processing step of downstream analysis to reduce the dimensions of data to hundreds [Tung *et al.*, 2017]. The challenge in dimensionality reduction for single-cell sequencing data lies in the preservation of the data global structure, which contains great biological significance. The better global structure makes the distribution of clusters on the 2D scatter plot obey the similarity of the biological characteristics of cell types, whereby the 2D scatter plot should be reliable. Unfortunately, so far, even nonlinear dimensionality reduction methods don't consider the global structures of single-cell data. Here we propose SGEN, a single-cell data dimensionality reduction neural network based on graph convolutional networks (GCN). We construct the graph of cells by the similarity relationship

*Contact Author

†Contact Author

between cells and adopt GCN to get the node aggregated embedding. Aggregated region grants GCN the ability to analyze the neighbor embedding information of samples, which makes the similar cell closer to each other on the 2D scatter plot.

Compared with existing dimensionality reduction methods used in this domain, we highlight three contributions:

- Our algorithm preserves the global structure of the data, which means the distance between cell clusters reflect the similarity of cell types.
- SGEN can be used as a parametric model to directly position new samples on the trained 2D scatter plot, whereby we can quickly detect the biological state of the new samples.
- SGEN can provide the fake labels of 2-dimensional cell embedding, which explicitly present the biological state of the cells, namely, the points closer to the centroid verge to the common biological status.

2 Related works

In recent years, dimensional reduction of single-cell sequencing data for visualization has been a popular research topic. Several traditional machine learning methods have been proposed to visualize the 2d distribution of cells for better biological analysis. Meanwhile, deep learning methods haven't been widely used for the visualization target.

t-distributed stochastic neighborhood embedding (t-SNE) [Laurens and Hinton, 2008] is currently the most commonly used technology in single-cell analysis. t-SNE has strong ability in preserving microstructure, but it is at the expense of its ability to preserve global structure [Wattenberg et al., 2016]. In other words, t-SNE can put similar cells close together on a 2D scatter plot, but it cannot put diverse cells far apart, which will make the position relations between cell clusters in the t-SNE plot unreliable [Wattenberg et al., 2016]. [Kobak and Berens, 2019] proposed three improvements for the traditional t-SNE to alleviate this problem, including PCA initialisation, a high learning rate, and multi-scale similarity kernels. The heavily optimized fourier-interpolated t-SNE (Fit-SNE) proposed by [Linderman et al., 2017] is widely used in single-cell data analysis because it greatly reduces the run time of t-SNE. PHATE [Moon et al., 2017], using the manifold distance to measure the difference of samples, can encode the relevant information with fewer dimensions via multidimensional scaling (MDS). With diffusion map, PHATE works well in tracking trends of the data [Haghverdi et al., 2016]. [Etienne et al., 2018] proposed UMAP, a dimensionality reduction model which greatly reduces running time, but it does not effectively separate clusters of cells, which means the distance between clusters cannot reflect the difference between cell types. scvis [Ding et al., 2018], as deep generative models, can preserve the global structure of data and greatly extract interpretation of projected structures, but the algorithm is time-consuming, and even the efficiency is not as good as t-SNE on small data sets.

In recent years, graph neural network(GNN) has been developed to learn the topological information of data, which

is widely used in the fields of social sciences[Kipf and Welling, 2017], knowledge graphs[Schlichtkrull et al., 2018], chemistry[Duvinaud et al., 2015]. In the case of fixed-size graphs, a series of convolutional neural networks based on the spectral representation of the graphs have been applied on the node classification. Specifically, Kipf & Welling[Kipf and Welling, 2017] proposed a simplified spectral neural network using 1-hop filters to address overfitting problem and minimize the number of operations.

3 Network architecture

SGEN is an encoder-decoder model(Figure 1). We aim to get a low-dimensional embedding that preserves enough information to construct the original gene expression. We construct the cells similarity graph for graph convolutional operation. Then, the topological aggregated features outputted by graph convolutional operation are processed via a fully connected auto-encoder. We construct the fake similarity graph and compute the Kullback-Leibler divergence between the true and fake graphs to get the graph construction loss. Besides, we get the fake cluster assignment of cells and compute the mean distance of data-centroid distance to get the data-centroid loss. Lastly, we use backpropagation to train single-cell sequencing graph embedding networks according to the expression reconstruction loss, graph construction loss and data-centroid loss.

4 Methodology

4.1 Feature selection

In our study, not all gene expression contributes to the single cell embedding cluster. We don't aim to focus on the zero expression genes. Any gene that has high dropout rate and high non-zero mean expression could potentially be a marker of some particular subpopulation. To analyze potential contribution of each gene g , we compute the fraction of zero counts

$$d_g = \frac{1}{n} \sum_i I(X_{ig} = 0) \quad (1)$$

and the mean log non-zero expression

$$m_g = \{\log_2 X_{ig} \mid X_{ig} > 0\} \quad (2)$$

where I is the counting function.

In order to select the genes that have special value for clustering. We intend to find the gene that have high mean log non-zero expression and high zero counts. However, there is a strong negative relationship between d_g and m_g across all the remaining genes. We use the formula to get the M-dimensional features for neural networks inputs:

$$d_g > \exp[-(m_g - b)] + 0.02 \quad (3)$$

where M is a hyperparameter to select a pre-specified number of contributive genes, b is the value we need to find for matching M . This process can be done through a binary search.

4.2 Graph construction

To reflect the local structure in the high-dimensional space, we define the relationship of point i to j according to the

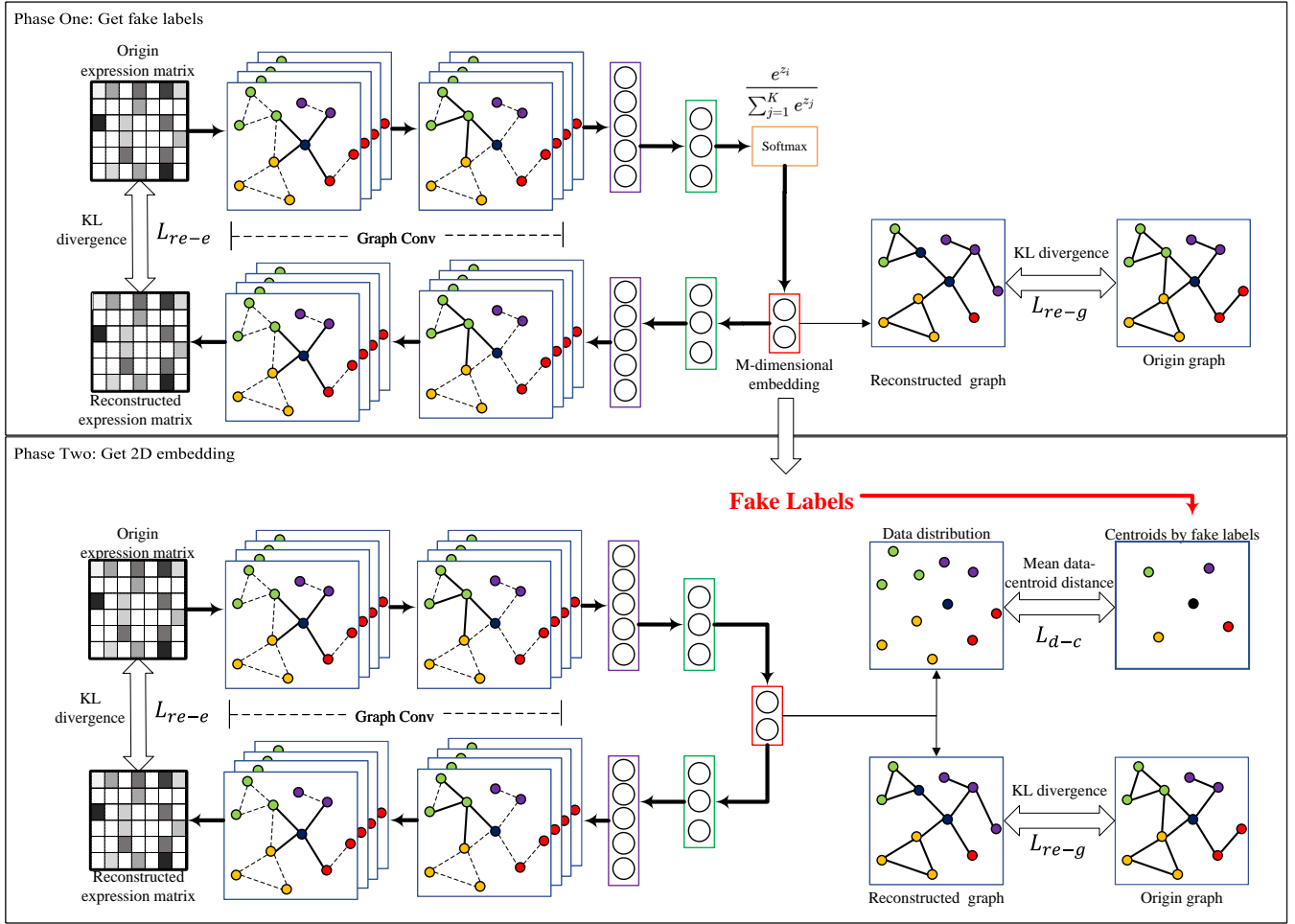


Figure 1: Network architecture of SGEN. The origin gene expression is inputted into network for reconstructed expression output. Different colored nodes in the graph represent cells of different categories. We get the low-dimensional embedding vector from the output of the encoder. The embedding vector are then used to compute the data-centroid loss and graph reconstruction loss.

notion of directional similarity introduced by SNE [Hinton and Roweis, 2002]. We construct the graph to measure similarity between each point. The node features of graph are defined by the normalization of the pre-specified number of contributive genes. We use the directional similarity to construct edges of the similarity graph.

$$p_{i|j} = \frac{\exp(-\|x_i - x_j\|^2/2\sigma_i^2)}{\sum_{k \neq i} \exp(-\|x_i - x_k\|^2/2\sigma_i^2)} \quad (4)$$

The variance σ_i^2 of Gaussian kernel, which is often set to 30, is chosen with the criterion that the perplexity of this probability distribution equals to a pre-defined hyperparameter. The perplexity is defined as:

$$\mathcal{P}_i = \exp\left(-\log(2) \sum_{j \neq i} p_{j|i} \log_2 p_{j|i}\right) \quad (5)$$

Because we only focus on the similarity of different points, we set $p_{i|i}$ as 0. For the computational convenience, we get the undirectional similarity A by $A = (P + P^T)/2$, where

P is the normalized directional similarity matrix, P^T is the transpose of matrix P .

4.3 Graph convolutional network

For previous deep learning methods, the gene expression is inputted into the fully connected layers to get the embedding, which don't consider the neighborhood information of points. For the GNN methods, the adjacent matrix is inputted into the GNN model to aggregate the adjacent node information. In this paper, we use GNN to learn the adjacent node information and node embedding features to analyze the similar points.

Given a graph $G = (V, E, A)$, where V is a finite set of $|V| = n$ nodes, E is a set of edges and $A \in \mathbb{R}^{n \times n}$ is an adjacency matrix encoding the connection weight between two nodes. For comprehension, we consider the graph convolution following general "message-passing" architecture:

$$H^{(l)} = F\left(A, H^{(l-1)}; \theta^{(l)}\right) \quad (6)$$

where $H^{(l)} \in \mathbb{R}^{n \times d}$ are the node embeddings after l steps of

graph convolution operation, F is the graph convolution operation which is known as the message propagation function, $H^{(l-1)}$ is the output of last convolution operation, $\theta^{(l)}$ is the trainable parameters.

Many implementations of message propagation function have been proposed to get the output of the graph convolution operation. A popular method is the graph convolution network [Kipf and Welling, 2017], which is implemented by linear transformations and ReLU non-linearities:

$$H^{(l)} = \text{ReLU} \left(\tilde{D}^{-\frac{1}{2}} \tilde{A} \tilde{D}^{-\frac{1}{2}} X^{(l-1)} W^{(l)} \right) \quad (7)$$

where $\tilde{A} = A + I_N$, $\tilde{D}_{ij} = \sum_j \tilde{A}_{ij}$ and $W^{(l)}$ is a trainable matrix. \tilde{D} is the degree matrix of \tilde{A} . $\tilde{D}^{-\frac{1}{2}} \tilde{A} \tilde{D}^{-\frac{1}{2}}$ is a renormalization trick which is introduced to alleviate the numerical instability and exploding/vanishing gradient problem.

4.4 Expression reconstruction loss

The encoder processes the inputted features to get the low-dimensional embedding. If the original features and the outputted features are the same, we could say that the low-dimensional features have the ability to represent the original features. Therefore, our target is that the reconstructed expression features should be as similar to original features as possible. The reconstruction loss is defined as:

$$L_{re-e} = KL(X, Y) \propto -\frac{1}{n} \sum_i x_i \log y_i \quad (8)$$

where X is the original expression features, Y is the reconstructed expression features. x_i and y_i are the i^{th} original data and reconstructed data, respectively.

4.5 Graph reconstruction loss

We adopt the main idea of t-SNE, which use a t-distribution with one degree of freedom as the low-dimensional similarity kernel:

$$q_{ij} = \frac{w_{ij}}{\sum_{k, k \neq i} w_{ik}}, w_{ij} = \frac{1}{1 + \|z_i - z_j\|^2} \quad (9)$$

where q_{ij} is the similarity between the 2-dimensional embedding of the i^{th} and the j^{th} points, z_i is the 2-dimensional embedding of the i^{th} point. Thus, we can get the similarity matrix based on the 2-dimensional embedding.

To ensure that the low-dimensional embedding remains the interactive similar relationship of the high-dimensional features, we minimize the Kullback-Leibler divergence between the low- and high- dimensional features:

$$L_{re-g} = \sum_{i,j} p_{ij} \log \frac{p_{ij}}{q_{ij}} \propto -\sum_{i,j} p_{ij} \log q_{ij} \quad (10)$$

where p_{ij} is the similarity between the original features of the i^{th} and the j^{th} points.

4.6 Data-centroid loss

Although previous methods can capture and visualize the low-dimensional structures, it's hard to distinguish local neighbor structures and the subordinate clusters. To analyze the local property of points carefully, we train another network and save the fake labels. The networks have the same

structure as SGEN and only adopt L_{re-e} and L_{re-g} . We input expression features and set the latent dimension as number of clusters. We activate the latent vector using softmax activation layer. Then, we get the latent vector as fake labels for single cells. The detailed information is shown in supplement materials (Figure S1).

Therefore, we can get the fake centroid of cells with the each cluster by the fake labels. We aim to minimize the mean distance between the 2D embeddings and centroids. Thus, the similar points will cluster together around the nearest centroid. Then we design a data-centroid loss function as follow:

$$L_{d-c} = \frac{1}{n} \sum_i^n \min_j \|x_i - c_j\|_2 \quad (11)$$

where n is the number of points, x_i is the 2-dimensional embedding of points, c_j is the 2-dimensional coordinates of the centroids computed according to the fake labels. The number of the cluster centroids is a hyperparameter, which we set to 80 in our model. To make it easier to converge, we update the centroid of cells every 5 epochs.

4.7 Loss function

We consider the expression reconstruction loss, graph reconstruction loss and data-centroid loss together. Thus the loss function of our method is defined as follows:

$$\text{Loss} = L_{re-e} + L_{re-g} + \lambda * L_{d-c} \quad (12)$$

where λ is hyperparameter that decides the influence of the data-centroid loss, which we set to 0.1 in our paper.

5 Experiments

5.1 Evaluation metric

- Fisher's ratio: The ratio of intra-cluster to inter-cluster scatter matrices can be used to formulate an effective criterion of cluster relationship, which is known as Fisher's ratio. The intra-cluster and inter-cluster scatter matrices are defined as:

$$S_W = \sum_c \sum_{i \in c} (y_i - \bar{Y}_c) (y_i - \bar{Y}_c)^T \quad (13)$$

$$S_B = \sum_c (Y_c - \bar{Y}) (Y_c - \bar{Y})^T \quad (14)$$

where \bar{Y}_c is the class-oriented average value, and \bar{Y} is the overall mean of the data. The ratio determining the class separability is defined as:

$$J_{B/W} = \text{tr} (S_W^{-1} S_B) = \text{tr} (S_B S_W^{-1}) \quad (15)$$

The larger $J_{B/W}$, the more compact points of the same clusters and the more sperate points of different clusters. We use the ratio to reveal the distribution of low-dimensional points.

- KNC: The fraction of k-nearest class(KNC) means in the original data, which are preserved as k-nearest class means in the embedding. This is computed for class means only and averaged across all classes. For all datasets, we set the k as 10. KNC quantifies the preservation of the mesoscopic structure.

- CPD: Spearman correlation between pairwise distances(CPD) in the high-dimensional space and in the embedding, which is computed with all cell pairs in the datasets among 1000 randomly chosen points. CPD quantifies preservation of the global, or macroscopic structure.

5.2 Datasets

In this study, we use four single-cell sequencing data for experiments.

[Tasic *et al.*, 2018] investigated the diversity of cell types across the adult mouse neocortex, collecting 23822 cells from two areas at distant poles of the mouse neocortex. In the dataset, 133 transcriptomic cell types are analyzed.

[Shekhar *et al.*, 2016] derived a digital expression matrix appreciably expressed genes across 27,499 cells after aligning reads, demultiplexing and counting UMIs. The dataset has identified 26 putative cell type clusters.

[Macosko *et al.*, 2015] analyzed transcriptomes from 44808 mouse retinal cells and identified 39 transcriptionally distinct cell populations

Furthermore, we use Samusik_01 dataset [Samusik *et al.*, 2016] to explain the function of GSEN in tracking Cell development trajectory. Samusik_01 dataset contain 86864 cells from 24 cell populations, which are all related to bone marrow hematopoiesis.

5.3 Parameter setting

We train our model for a maximum of 1000 epochs using Adam [Kingma and Ba, 2015]. For each epoch, we set the size of batched training data as 1024. For the learning rate parameters, we set the initial learning rate as 0.001 and the learning rate reduce factor as 0.5. The learning rate will decrease by learning rate reduce factor if the training loss does not decrease for 10 consecutive epochs. When the learning rate is equal to $1e-8$, the training procedure will stop. Small change of the other parameters did not change the results much. We set the weight decay and dropout as 0.01 and 0.1 respectively. For baseline models, we set the parameters same as their original papers.

We run our experiments on a Ubuntu server with NVIDIA GTX 2080Ti GPU with memory 12 GB. The initial weights and bias use default setting in PyTorch.

5.4 Preservation results

We compare our method with other baseline methods on Tasic, bipolar and retina datasets. The detailed results are listed in the Table 1. For the Tasic and retina datasets, GSEN performs the best on Fisher’s ratio(FR), KNC and CPD. For the bipolar dataset, SGEN gets the second best KNC and CPD.

In general, SGEN performs well in CPD on the three datasets, which means that SGEN can highly preserve the global structure of cells in the low-dimensional embedding. The relationship between different clusters can be well reflected in the 2D visualization.

Besides, SGEN gets better FR on single-cell datasets. On the Tasic and retina datasets, we get the best performance,

Table 1: Performance of our method and other baseline methods on Tasic, bipolar and retina dataset. The italic and bold font indicates the best and the second best among compared methods.

Datasets	Method	FR	KNC	CPD
Tasic	t-SNE	1.3468	0.6910	0.5070
	UMAP	2.3546	0.6684	<i>0.5133</i>
	scvis	<i>2.4530</i>	<i>0.7308</i>	0.4612
	SGEN	2.4688	0.7376	0.6214
Bipolar	t-SNE	0.0251	0.4462	0.5003
	UMAP	0.0773	0.5115	0.5881
	scvis	<i>0.07538</i>	0.6346	0.6652
	SGEN	0.05098	<i>0.5150</i>	<i>0.6588</i>
Retina	t-SNE	0.0087	0.7615	0.7275
	UMAP	0.0165	0.7436	0.8982
	scvis	<i>0.0194</i>	<i>0.7769</i>	<i>0.9140</i>
	SGEN	0.0224	0.7923	0.9155

which can be seen from Figure 3 that different cells are separated apart clearly and similar cells are pulled in together. Without the cell labels, we can easily get the cell type for better biological research. The results of FR reflect that our methods can perform well on the preservation of local structure information.

Furthermore, our method gets the highest KNC across the Tasic and retina datasets. The neighbor clusters of different cell type are well preserved through SGEN. Although scvis gets the performance on the metrics, too many scattered points exist in the plot and the distribution of different cells aren’t clear. When the color of the points are the same in the plot, it’s hard to tell which clusters the cells should belong to.

5.5 Loss influence

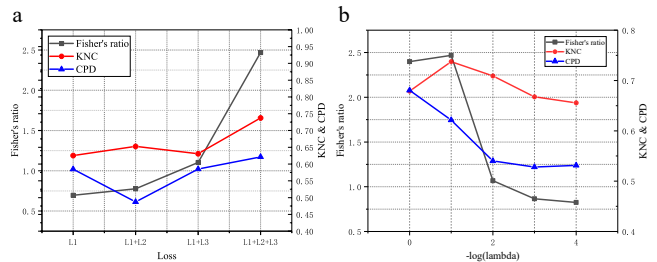


Figure 2: The influence of loss setting on embedding quality on the Tasic dataset. (a) Embedding quality results of different loss combination. L1, L2 and L3 represent L_{re-e} , L_{re-g} and L_{d-c} , respectively. (b) Embedding quality results of different λ , where λ decides the influence of the data-centroid loss.

We explain the function of each loss designed in GSEN. The detailed results can be seen in Figure 2.

From Figure 2a, Fisher’s ratio increases a lot when L_{re-g} and L_{d-c} are added to constraint the converge of the network. Each of L_{re-g} and L_{d-c} can benefit KNC. Although

L_{re-g} makes GSEN perform worse at CPD, integration of L_{re-g} and L_{d-c} can boost the model performance. It can be demonstrated from Figure 2 that L_{re-g} and L_{d-c} are relatively independent and have complementary effects for GSEN.

From Figure 2b, L_{d-c} will constraint the model to preserve more local structure of cells distribution. Besides, λ can benefit the preeservation of global structure. However, when λ is too large the KNC will begin to decrease, which means that our model will damage mesoscopic structure. To make GSEN focus on local, mesoscopic and global structure together, we often set λ to 0.1.

5.6 Visualization comprison

In the Tasic data, there are three main groups of cells, excitatory neurons (cold colours), inhibitory neurons (warm colours), and non-neural cells such as astrocytes or microglia (grey/brown colours). The three groups have subclusters, which are again composed of several similar cell types. This hierarchy can be clearly seen from SGEN (Figure 3d), but it is almost invisible from UMAP (Figure 3b). t-SNE (Figure 3a) and scvis(Figure 3c) can roughly indicate the three types of excitatory neurons, inhibitory neurons, and non-neural cells, but the distance between subclusters and between cell clusters within a subclusters cannot reflect the difference of cell types, misrepresenting the hierarchy of cell types. For Bipolar and Retina dataset, scvis has so many out-of-cluster points that cannot be placed in the corresponding cluster(Figure 3g, k). Although UMAP can tightly cluster the cell in common types, as in the Tasic dataset, it does not present the global structure of the data (Figure 3f, j), and the position relation between clusters is dependent on the random initial condition. Both SGEN and t-SNE (the current mainstream applications in this field) have performed well(Figure 3e, h, i, l).

5.7 Biological analysis

In order to further verify that SGEN can make the distance of point clusters on the 2D scatter plot obey the difference of cell types, we used SGEN to reduce the dimension to 2-dimension on the Samusik.01 dataset(Figure 4). To our surprise, we found that the position of corresponding cell clusters on the 2D scatter plot can form the developmental trajectory of cells. First of all, it is obvious that the subsets belonging to B cells and T cells are all close together without overlapping. Next, a differentiation trajectory was observed. Hematopoietic stem cells (HSCs) and multipotent progenitors (MPPs) as stem cells have similar expression characteristics and exist partial overlap. HSCs can differentiate into common myeloid progenitors (CMPs). CMPs then led to Granulocyte -myeloid progenitors (GMPs), which has two directions of differentiation, classical monocytes and intermediate monocytes, and continuous distribution points between classical monocytes and CMPs may be the cells in the process of differentiation. The above cell differentiation processes are shown in a continuous track on the 2D scatter plot. Moreover, we can further confirm that SGEN makes the dissimilar cells far away while the similar cell close to each other on the 2D scatter plot, for example, nonclassical monocytes and PDCs are far away from the surrounding clusters, respectively.

6 Conclusion

In this study, we develop a novel deep learning model based GCN to get the 2D embedding for the visualization of single-cell data. We construct the graph by the similarity relationship between cells and adopt GCN to analyze the neighbor embedding information of samples, which makes the similar cell closer to each other on the 2D scatter plot. The results show SGEN achieves obvious 2D distribution and preserves the high-dimensional relationship of different cells. Furthermore, we use 2D embedding of GSEN for biological research and get the cell information that is consistent with the biological knowledge from existing literatures.

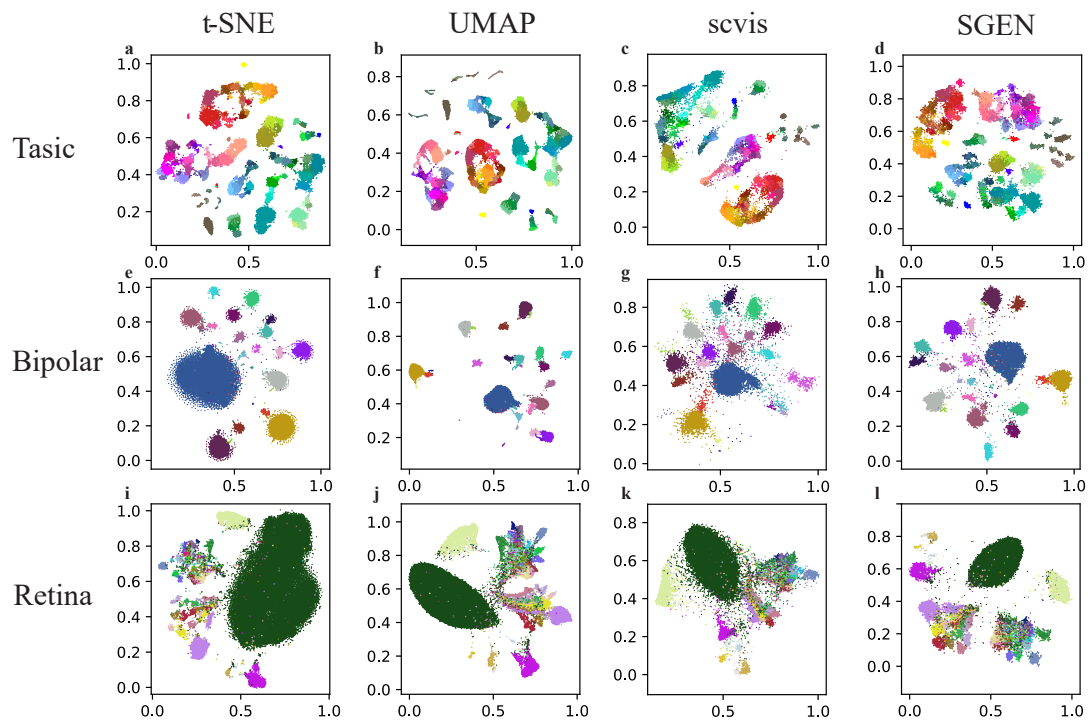


Figure 3: 2D visualization of t-SNE, UMAP, sevis and SGEN on Tasic, bipolar and retina datasets, respectively. The color of different cells in the Tasic dataset are set according to the similarity, which means similar cell types share similar colors. The color of clusters in the bipolar and retina datasets are randomized. All the 2D embedding points are normalized between 0 and 1 for better comprison.

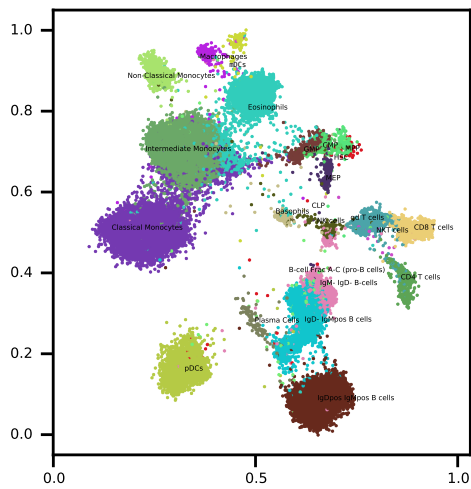


Figure 4: SGEN embeddings of Samusik_01 dataset, the color of clusters is randomized. The cell types are annotated at the centroids of corresponding clusters.

References

- [Ding *et al.*, 2018] Jiarui Ding, Anne Condon, and Sohrab P. Shah. Interpretable dimensionality reduction of single cell transcriptome data with deep generative models. *Nature Communications*, 9(1):2002, 2018.
- [Duvenaud *et al.*, 2015] David K Duvenaud, Dougal Maclaurin, Jorge Iparraguirre, Rafael Bombarell, Timothy Hirzel, Alán Aspuru-Guzik, and Ryan P Adams. Convolutional networks on graphs for learning molecular fingerprints. In *Advances in neural information processing systems*, pages 2224–2232, 2015.
- [Etienne *et al.*, 2018] Etienne, Becht, Leland, McInnes, John, Healy, Charles-Antoine, Dutertre, Immanuel, and W and. Dimensionality reduction for visualizing single-cell data using umap. *Nature Biotechnology*, 2018.
- [Franke *et al.*, 2006] Lude Franke, Harm Van Bakel, Like Fokkens, Edwin D De Jong, Michael Egmont-Petersen, and Cisca Wijmenga. Reconstruction of a functional human gene network, with an application for prioritizing positional candidate genes. *The American Journal of Human Genetics*, 78(6):1011–1025, 2006.
- [Gawad *et al.*, 2016] Charles Gawad, Winston Koh, and Stephen R. Quake. Single-cell genome sequencing: current state of the science. *Nature Reviews Genetics*, 2016.
- [Grün *et al.*,] Dominic Grün, Anna Lyubimova, Lennart Kester, Kay Wiebrands, Onur Basak, Nobuo Sasaki, Hans Clevers, and Alexander Van Oudenaarden. Single-cell messenger rna sequencing reveals rare intestinal cell types. *Nature*.
- [Haghverdi *et al.*, 2016] Laleh Haghverdi, Maren Büttner, F Alexander Wolf, Florian Buettner, and Fabian J Theis. Diffusion pseudotime robustly reconstructs lineage branching. *Nature Methods*, 2016.
- [Hinton and Roweis, 2002] Geoffrey E. Hinton and Sam T. Roweis. Stochastic neighbor embedding. In Suzanna Becker, Sebastian Thrun, and Klaus Obermayer, editors, *Advances in Neural Information Processing Systems 15 [Neural Information Processing Systems, NIPS 2002, December 9-14, 2002, Vancouver, British Columbia, Canada]*, pages 833–840. MIT Press, 2002.
- [Hubert and Arabie, 1985] Lawrence Hubert and Phipps Arabie. Comparing partitions. *Journal of classification*, 2(1):193–218, 1985.
- [Kingma and Ba, 2015] Diederik P Kingma and Jimmy Lei Ba. Adam: A method for stochastic gradient descent. In *ICLR: International Conference on Learning Representations*, 2015.
- [Kipf and Welling, 2017] Thomas N. Kipf and Max Welling. Semi-supervised classification with graph convolutional networks. In *5th International Conference on Learning Representations, ICLR 2017, Toulon, France, April 24-26, 2017, Conference Track Proceedings*, 2017.
- [Kobak and Berens, 2019] Dmitry Kobak and Philipp Berens. The art of using t-sne for single-cell transcriptomics. *Nature Communications*, 10(1), 2019.
- [Laurens and Hinton, 2008] Van Der Maaten Laurens and Geoffrey Hinton. Visualizing data using t-sne. *Journal of Machine Learning Research*, 9(2605):2579–2605, 2008.
- [Linderman *et al.*, 2017] George C Linderman, Manas Rachh, Jeremy G Hoskins, Stefan Steinerberger, and Yuval Kluger. Efficient algorithms for t-distributed stochastic neighborhood embedding. 2017.
- [Macosko *et al.*, 2015] Evan Z Macosko, Anindita Basu, Rahul Satija, James Nemesh, Karthik Shekhar, Melissa Goldman, Itay Tirosh, Allison R Bialas, Nolan Kamitaki, Emily M Martersteck, et al. Highly parallel genome-wide expression profiling of individual cells using nanoliter droplets. *Cell*, 161(5):1202–1214, 2015.
- [Moon *et al.*, 2017] Kevin R Moon, David van Dijk, Zheng Wang, William Chen, Matthew J Hirn, Ronald R Coifman, Natalia B Ivanova, Guy Wolf, and Smita Krishnaswamy. Phate: a dimensionality reduction method for visualizing trajectory structures in high-dimensional biological data. *BioRxiv*, page 120378, 2017.
- [Samusik *et al.*, 2016] Nikolay Samusik, Zinaida Good, Matthew H Spitzer, Kara L Davis, and Garry P Nolan. Automated mapping of phenotype space with single-cell data. *Nature methods*, 13(6):493–496, 2016.
- [Schlichtkrull *et al.*, 2018] Michael Schlichtkrull, Thomas N Kipf, Peter Bloem, Rianne Van Den Berg, Ivan Titov, and Max Welling. Modeling relational data with graph convolutional networks. In *European Semantic Web Conference*, pages 593–607. Springer, 2018.
- [Shekhar *et al.*, 2016] Karthik Shekhar, Sylvain W Lapan, Irene E Whitney, Nicholas M Tran, Evan Z Macosko, Monika Kowalczyk, Xian Adiconis, Joshua Z Levin, James Nemesh, Melissa Goldman, et al. Comprehensive classification of retinal bipolar neurons by single-cell transcriptomics. *Cell*, 166(5):1308–1323, 2016.
- [Stubbington *et al.*, 2017] Michael J. T. Stubbington, Orit Rozenblatt-Rosen, Aviv Regev, and Sarah A. Teichmann. Single-cell transcriptomics to explore the immune system in health and disease. *Science*, 358(6359):58, 2017.
- [Tasic *et al.*, 2018] Bosiljka Tasic, Zizhen Yao, Lucas T Graybuck, Kimberly A Smith, Thuc Nghi Nguyen, Darren Bertagnolli, Jeff Goldy, Emma Garren, Michael N Economo, Sarada Viswanathan, et al. Shared and distinct transcriptomic cell types across neocortical areas. *Nature*, 563(7729):72–78, 2018.
- [Tung *et al.*, 2017] Po-Yuan Tung, John D Blischak, Chiaowen Joyce Hsiao, David A Knowles, Jonathan E Burnett, Jonathan K Pritchard, and Yoav Gilad. Batch effects and the effective design of single-cell gene expression studies. *Scientific reports*, 7:39921, 2017.
- [Wang *et al.*, 2014] Yong Wang, Jill Waters, Marco L Leung, Anna Unruh, Whijae Roh, Xiuqing Shi, Ken Chen, Paul Scheet, Selina Vattathil, Han Liang, et al. Clonal evolution in breast cancer revealed by single nucleus genome sequencing. *Nature*, 512(7513):155–160, 2014.
- [Wattenberg *et al.*, 2016] Martin Wattenberg, Fernanda Viégas, and Ian Johnson. How to use t-sne effectively. *Distill*, 1(10), 2016.
- [William *et al.*, 1971] William, M., and Rand. Objective criteria for the evaluation of clustering methods. *Journal of the American Statistical Association*, 66(336):846–850, 1971.
- [Yoon *et al.*, 2011] Hwan Su Yoon, Dana C. Price, Ramunas Stepanauskas, Veeran D. Rajah, Michael E. Sieracki, William H. Wilson, Eun Chan Yang, Siobain Duffy, and Debashish Bhattacharya. Single-cell genomics reveals organismal interactions in uncultivated marine protists. *Science*, 332(6030):714–7, 2011.